European Heart Journal (2009) **30**, 2241–2248
doi:10.1093/eurheartj/ehp252

Magnetic resonance investigations in Brugada syndrome reveal unexpectedly high rate of structural abnormalities

Oronzo Catalano[1]*, Serena Antonaci[1], Guido Moro[2], Maria Mussida[1], Mauro Frascaroli[2], Maurizia Baldi[2], Franco Cobelli[1], Paola Baiardi[5], Janni Nastoli[3], Raffaella Bloise[3], Nicola Monteforte[3], Carlo Napolitano[3], and Silvia G. Priori[3,4]

[1]Division of Cardiology, IRCCS Fondazione Salvatore Maugeri, via Maugeri 8, 27100 Pavia, Italy; [2]Division of Radiology, IRCCS Fondazione Salvatore Maugeri, Pavia, Italy; [3]Molecular Cardiology, IRCCS Fondazione Salvatore Maugeri, Pavia, Italy; [4]Department of Cardiology, University of Pavia, Pavia, Italy; and [5]Consorzio Valutazioni Biologiche e Farmacologiche, IRCCS Fondazione Salvatore Maugeri and University of Pavia, Pavia, Italy

Received 28 April 2008; revised 20 April 2009; accepted 25 May 2009; online publish-ahead-of-print 26 June 2009

Aims Recent data suggest that sub-clinical structural abnormalities may be part of the Brugada syndrome (BrS) phenotype, a disease traditionally thought to occur in the structurally normal heart. In this study, we carried out detailed assessment of cardiac morphology and function using cardiac magnetic resonance imaging (CMRI).

Methods and results Thirty consecutive patients with BrS were compared with 30 sex- (26/4 male/female), body surface area- (± 0.2 m^2), and age-matched (± 5 years) normal volunteers. CMRI exam included long- and short-axis ECG-gated breath-hold morphological T1-TSE sequences for fatty infiltration and cine-SSFP sequences for kinetic assessment. Fatty infiltration was not found in any subject. Patients with BrS compared with normal subjects showed higher incidence of mild right ventricle (RV) wall-motion abnormalities [15 (50%) vs. 5 (17%) subjects ($P = 0.006$) with reduced radial fractional shortening in more than two segments], reduction of outflow tract ejection fraction ($49 \pm 11\%$ vs. $55 \pm 10\%$; $P = 0.032$), enlargement of the inflow tract diameter (46 ± 4 vs. 41 ± 5 mm, $P < 0.001$ in short-axis; 46 ± 4 vs. 42 ± 5 mm, $P = 0.001$ in four-chamber long-axis view) and area (22 ± 2 vs. 20 ± 3 cm^2; $P = 0.050$), and of global RV end-systolic volume (34 ± 10 vs. 30 ± 6 mL/m^2; $P = 0.031$) but comparable outflow tract dimensions, global RV end-diastolic volume, left ventricle parameters, and atria areas.

Conclusion CMRI detects a high prevalence of mild structural changes of the RV, and suggests further pathophysiological complexity in BrS. Prospective studies to assess the long-term evolution of such abnormalities are warranted.

Keywords Brugada syndrome • Cardiac magnetic resonance imaging • Sudden cardiac death • *SCN5A*

Introduction

The Brugada syndrome (BrS) is an inherited cardiac disease associated with a high risk of ventricular tachyarrhythmias and sudden cardiac death in young and otherwise healthy adults. It is characterized by an electrocardiographic pattern of complete or incomplete right bundle branch block (RBBB) and by a dynamic ST-segment elevation in the right precordial leads (V_1–V_3).[1–3] BrS has been linked to mutations in the *SCN5A* gene located on chromosome 3, which encodes for the alpha subunit of the cardiac sodium channel.[4–8] More recently, additional ion channels and ion channel-regulating genes have been identified. Therefore, for many years BrS has been considered a purely electrical disease even if, more recently, some authors have suggested the presence of morphological and functional abnormalities in patients with BrS, predominantly located in the right ventricle (RV) and specifically in the outflow tract (RVOT).[9–13]

Cardiac magnetic resonance imaging (CMRI), thanks to its high spatial resolution, the lack of interferences with the extracardiac structures, the possibility of acquiring kinetic images, and the

* Corresponding author. Tel: +39 (0) 382592611, Fax: +39 (0) 382592099, Email: oronzo.catalano@fsm.it

ability to provide tissue characterization, allows a high-quality assessment of cardiac morphology and function. CMRI is an accurate and reproducible tool for evaluating the RV, which is often difficult to assess with other imaging techniques. So far, only one study evaluated CMRI features of BrS patients.[14] Unfortunately, only standard axial sections were used for measurements, which are now considered only a part of CMRI acquisition protocols for arrhythmogenic cardiac diseases assessment.[15]

Here, we aimed at performing detailed quantification of several CMRI parameters in a cohort of consecutive patients suffering from BrS to further exploit the hypothesis that mild or subclinical structural abnormalities may be present in this disease.

Methods

Study design and population

Thirty consecutive BrS patients were included in the study and were compared with 30 sex- (26/4 male/female), body surface area- (BSA; ± 0.2 m^2), and age-matched (± 5 years) normal volunteers (mean BSA: 1.87 $\pm$ 0.14 vs. 1.86 $\pm$ 0.18 m^2; mean age: 39 $\pm$ 12 vs. 38 $\pm$ 11 years, respectively). Control subjects were recruited among our hospital workers; 30 out of 32 contacted subjects adhered to our request. Exclusion criteria for normal volunteers were the presence of signs or symptoms of cardiac diseases, hypertension, diabetes, smoking (more than 10 cigarettes a day for more than 10 years), or being engaged in competitive sports. At the end of recruitment, independently from the original matching, we checked for the best matching in terms of age and BSA. Study sample size estimation was based on a conservative interpretation of a previous study by Bellenger *et al.*,[16] suggesting a minimum sample size of 10–15 patients to detect significant differences in the left ventricle (LV) parameters.

Diagnosis of BrS was based on the criteria reported in the consensus conference.[3] The presence/absence of spontaneous ECG pattern was assessed on resting ECG and with standard positioning of right precordial leads with no upper displacement. Arrhythmogenic right ventricle cardiomyopathy (ARVC) was carefully excluded with electrocardiographic and morphological assessments and no patient with >1 major or >2 minor criteria for ARVC diagnosis was included. Moreover, family history of ARVC was ruled out up to the second-degree relatives in order to try to avoid the possibility of recessive variants.

The study was approved by the Institutional Review Board. An informed consent to undergo CMRI was signed by all subjects.

Molecular analysis

DNA was extracted by means of standard procedures. The entire open reading frame of the *SCN5A* gene was PCR-amplified using specific primer pairs.[6] Each amplicon was analysed using high-performance liquid chromatography (Wave, Transgenomic, Omaha, NE, USA) with at least two fragment-specific melting temperatures. Abnormal chromatograms were directly sequenced or cloned (Topo-TA cloning, Invitrogen, Milan, IT, USA) and sequenced on both strands with an automated DNA analyzer (ABI Prism 310, Applied Biosystems, Foster City, CA, USA). A panel of 400 healthy individuals (800 alleles) was used as control.

Magnetic resonance imaging

CMRI study was performed using a 1.0-Tesla scanner with a dynamic gradient of 20 mT (Magneton Harmony, Siemens, Erlangen, Germany) and a phased-array cardiac coil. In all subjects, we acquired morphological and dynamic images of the heart in the long-axis (two-, three-, and four-chambers) as well as in the short-axis view [a stack of 6–10 slices from atrioventricular (AV) valvular plane to the apex]. In BrS patients two stacks of oblique axial planes with four to five planes parallel to the four-chamber long-axis plane, covering the inflow of the RV, and four to five planes parallel to the three-chamber long-axis plane, covering the outflow, were also acquired. ECG-gated cine images were obtained using a steady-state free procession dynamic gradient-echo sequence (repetition time 29 ms; time of echo 1.5 ms; flip angle 52°; matrix 236 × 256; FOV 236 × 280 mm; pixel 1.0 × 1.1 mm; slice thickness 8 mm). For morphological assessment, we used a T1-weighted TSE sequence [repetition time 1563 $\pm$ 317 (774–2122) ms; time of echo 7.7 ms; flip angle 180°; matrix 164 × 256; FOV 260 × 320 mm; pixel 1.6 × 1.3 mm; slice thickness 8 mm]. CMRI study required repeated respiratory breath-holds and lasted for about 25 min.

Images analysis

Off-line images analysis was performed by two experienced readers (O.C. and S.A.), blind with respect to clinical status of the subjects.

Regional contractility (hypokinesis, akinesis, dyskinesia) of the LV on the cine images and fatty infiltration (high-intensity signal within myocardium) of both ventricles on T1-weighted TSE images were visually identified by consensus of the two readers.

RV regional contractility was quantitatively assessed, as described in *Figure 1*, by evaluating radial fractional shortening [(diastolic radius − systolic radius)/diastolic radius × 100%] in each of eight segments in which RV-free wall was divided (three basal, three mid-ventricular, and two apical). We identified segments with reduced contractility as those with a fractional shortening value under the 25th percentile

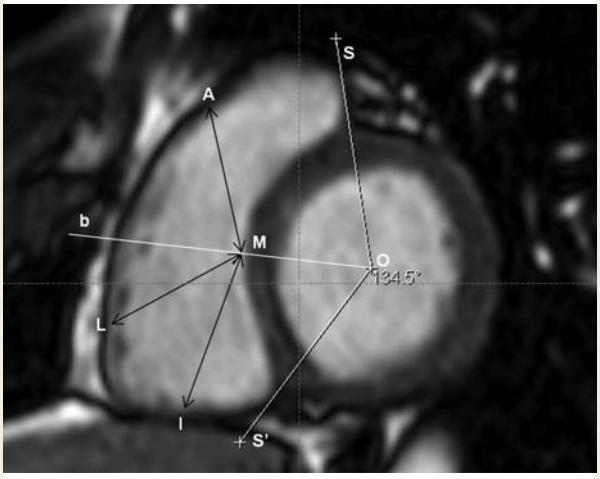

Figure 1 Assessment of right ventricle (RV) wall motion contractility as radial fractional shortening [(diastolic radius − systolic radius)/diastolic radius × 100%]. The middle point of the RV subendocardial contour of the interventricular septum (M), identified by the bisector line (b) of the angle subtending the interventricular septum itself with vertex in the centre of left ventricle cavity (SOS'), was the reference for the RV free wall excursion measurements. Fractional shortening of the distance (radius) from M to the middle subendocardial point of the anterior (A), lateral (L), and inferior (I) free wall was obtained at basal and mid-ventricular level, and from M to the anterior and inferior RV free wall at apical level (eight segments in total). Diastolic assessment at basal level is shown.

of the segment-specific pooled values (BrS plus normal subjects). Moreover, tricuspidal annular plane systolic excursion (TAPSE), that is RV apical to base shortening was evaluated to explore longitudinal shortening component of RV inflow tract (RVIT) contraction.

A series of mono-dimensional measurements of both LV and RV were obtained at end-diastole, about 1 cm below the AV valve plane (*Figure 2*). The area of both atria was measured at end-systole on the four-chamber slice. On the short-axis slice closest to tricuspidalic plane with RVIT and RVOT chambers in full continuity, we measured the areas of both inflow and outflow parts of the RV (*Figure 3*).

Quantitative analysis of cine images was performed using commercial software (ARGUS, Siemens). Through semi-automatic contouring of endocardial and epicardial borders end-diastolic volumes (EDV), end-systolic volumes (ESV), ejection fraction (EF), and mass of both the LV and the RV were calculated. EDV and ESV, independently for the two ventricles, were defined by visually assessing the frames with the greatest and the smallest cavity areas using a short-axis slice at mid-ventricular level. The most basal slice included in the analysis was that with the outflow tract no longer visible for the LV, and with the inflow and the outflow chambers in full continuity for the RV.

Regional volumes and ejection fraction of RVIT and RVOT were also assessed using the same commercial software but with manual tracing of endocardial border. Supraventricular crista, the moderator band, the anterior papillary muscle, and the anterior cuspid of tricuspid valve were the anatomic markers used to distinguish the inflow part from the outflow part of RV cavity.

Statistical analysis

Categorical variables are presented as counts or percentages, quantitative variables as means $\pm$ SD. Student's paired *t*-test was used for comparison of quantitative variables. Pearson's χ^2 was used to test differences of categorical variables. $P < 0.05$ (two-sided) was considered statistically significant in all tests. Bonferroni correction was applied to manage multiple testing when we analysed differences about several cardiac segments, areas, and volumes (26 variables,

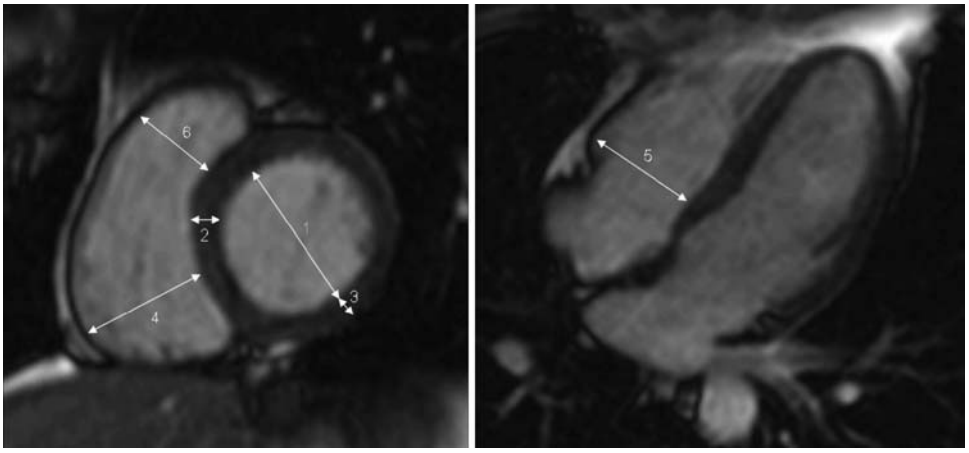

Figure 2 Assessment of right and left ventricle mono-dimensional parameters (end-diastole). 1 = left ventricle end-diastolic diameter; 2 = interventricular septum thickness; 3 = posterior wall thickness; 4 = right ventricle inflow tract diameter (short-axis); 5 = right ventricle inflow tract diameter (four-chamber long-axis); 6 = right ventricle outflow tract diameter.

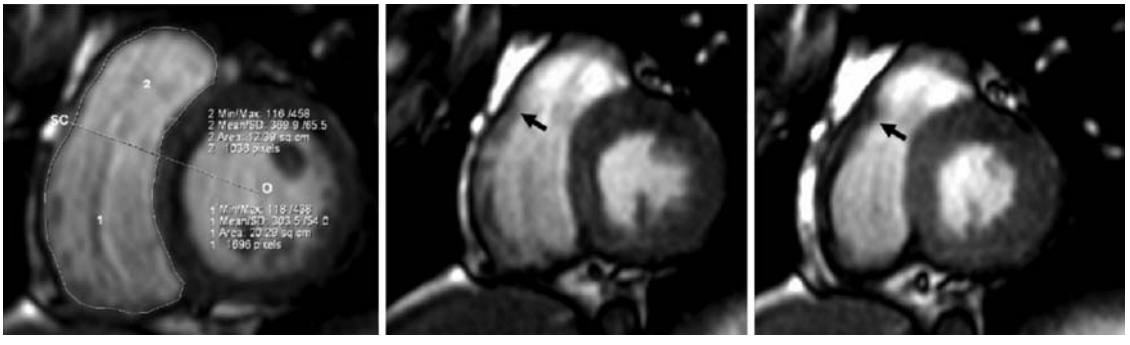

Figure 3 Assessment of RV inflow and outflow tracts area at end-diastole (left image) on the short-axis slice closest to tricuspidalic plane with inflow and outflow chambers in full continuity. Partition line was considered that passing through the supraventricular crista (SC) and the centre of the LV (O). SC position was verified by watching at the mid-systolic and end-systolic frames (arrows on the central and right images).

$P < 0.002 = 0.05/26$). Conditional logistic regression was used to investigate the association between BrS diagnosis (dependent variable) and RV regional contractility, simultaneously introduced into the model as eight covariates (differences between the case and the control values for the eight RV segments).

To assess intra- and inter-observer reproducibility of RVIT diameter (representative of all mono-dimensional measures) and of radial fractional shortening assessments, two blinded investigators (O.C. and S.A.) evaluated 20 randomly selected subjects among the study population (10 subjects, equal to 80 segments, for radial fractional shortening), and one of them repeated the measurements at least 1 week after the first evaluation. We calculated Bland–Altman mean difference (bias) and coefficients of repeatability (CoR = 1.96 × sqrt (2) × sw; where sw is the within-subject SD). We approached the problem of multiple segments per patient by following the method described by Bland–Altman in the case of multiple observations per individual.[17] RVIT diameter intra- and inter-observer mean difference (bias) were 0 and 0 mm, with CoR of 2.5 and 3.5 mm, respectively. Radial fractional shortening intra- and inter-observer biases were −1 and 1%, with CoRs of 18 and 23%, respectively. Bland–Altman plots are shown as Supplementary material online.

Results

The clinical, electrocardiographic, and genetic characteristics of patients with BrS are listed in *Table 1*. One-quarter of cases had a positive family history for sudden cardiac death (8/30, 27%) and syncope was reported (5/30, 17%) in patients. Standard 12-lead ECG showed spontaneous coved-type pattern in 10 (33%) patients, while the remaining had a diagnostic type 1 ECG pattern upon challenge with class Ic drug (Ajmaline 1 mg/kg i.v.). AV conduction delay and a complete or incomplete RBBB were present in 4 (13%) and 26 (87%) of controls and patients, respectively.

Table 1 Clinical, electrocardiographic, and genetic characteristics of patients with the Brugada syndrome

Patient number	Age/Sex	Family history	Symptoms	Standard 12-lead ECG			*SCN5A* mutations
				Spontaneous Type 1 pattern	AV conduction delay	RBB	
1	36/M	SCD	No	No	No	Incomplete	W1095X
2	41/M	No	No	No	No	No	R1512W[a]
3	23/F	SCD	No	No	No	Incomplete	No
4	57/M	No	Syncope	Yes	Yes	Complete	No
5	34/M	SCD	No	No	Yes	Complete	R1316X
6	43/M	BrS	No	No	No	Complete	No
7	26/M	No	No	Yes	No	No	No
8	28/M	No	No	Yes	No	Complete	No
9	49/M	No	No	No	No	Incomplete	No
10	58/M	No	No	Yes	No	Incomplete	No
11	49/M	No	No	Yes	Yes	No	V1405M
12	33/M	No	No	No	Yes	Incomplete	K1236X; V1279I
13	24/M	No	No	No	No	Incomplete	No
14	37/M	SCD	No	No	No	Incomplete	No
15	46/M	No	No	No	No	Incomplete	No
16	14/M	No	No	No	No	Complete	S303+6X
17	34/M	No	No	No	No	Incomplete	No
18	47/F	SCD	No	No	No	Incomplete	No
19	45/M	SCD	No	No	No	Complete	No
20	40/M	No	Syncope	No	No	Incomplete	No
21	31/M	No	No	Yes	No	Complete	G1420D
22	55/M	No	No	Yes	No	Incomplete	No
23	34/M	No	No	No	No	No	No
24	36/M	Syncope	Syncope	Yes	No	Complete	R367C[a]
25	29/M	No	Syncope	Yes	No	Incomplete	No
26	32/M	SCD	No	No	No	Complete	No
27	37/F	SCD	No	No	No	Incomplete	L749P
28	43/M	No	No	Yes	No	Complete	No
29	68/F	No	Syncope	No	No	Incomplete	No
30	37/M	No	No	No	No	Incomplete	No

SCD, sudden cardiac death; BrS, Brugada syndrome; AV, atrioventricular.
[a]Previously published.

Genetic screening identified a mutation in the *SCN5A* gene in nine patients (30%). Four mutations were nonsense or frame-shift leading to a truncated protein. Among the remaining five mutations, two were already reported in the literature (www.fsm.it/cardmoc). One patient was a compound heterozygous of two novel mutations, one truncation and one missense.

Wall motion assessment

At CMRI evaluation, none of patients or normal subjects showed fatty infiltration of the RV or LV. However, a significant high percentage of BrS patients presented with mild RV wall motion abnormalities in more than two segments [15 (50%) vs. 5 (17%) subjects; Pearson's χ^2: $P = 0.006$]. Analysis of RV regional contractility showed an association between BrS diagnosis and segmental contractility (−2 log-likelihoods model fitting: $P = 0.044$); with a higher risk of BrS in subjects with reduced function in the anterior-apical segment [$P = 0.041$; OR 6.8 (95% CI 1.1–41.7)], in the outflow, and in the inferior mid-ventricular segment [$P = 0.051$; OR 4.92 (95% CI 1–24.4)] in the inflow. An example of abnormal RV contractility in a patient with BrS is shown as Supplementary material online. LV segmental contractility was normal in the whole study population. There was no association between RV wall motion abnormalities and complete or any degree RBB (Pearson' χ^2: $P = 0.18$ and 0.14, respectively).

Right and left ventricle morphology

LV and RV dimensional and functional parameters as well as atrial areas are listed in *Table 2*. Patients with BrS showed larger RV ESV (34 ± 9 vs. 30 ± 6 mL/m^2; $P = 0.031$) but comparable RV EDV, EF, and mass respect to normal volunteers. LV assessment disclosed only slight interventricular septum thickening in BrS patients (9.5 ± 1.1 vs. 9.0 ± 1.1; $P = 0.030$), while there was no difference in terms of diameter, volumes, function, and mass. The area of both atria was similar in the two groups also.

Patients with BrS showed significant enlargement of the RVIT diameter in the short-axis view (46 ± 4 vs. 41 ± 5 mm,

Table 2 Ventricular and atrial parameters of patients with the Brugada syndrome and of normal volunteers at cardiac magnetic resonance imaging

	Brugada syndrome patients	Normal volunteers	*P*-value
Left ventricle			
End-diastolic volume (mL/m^2)	61 ± 10	59 ± 9	0.495
End-systolic volume (mL/m^2)	22 ± 6	21 ± 5	0.510
Ejection fraction (%)	64 ± 6	64 ± 6	0.819
Mass (g/m^2)	37 ± 11	33 ± 10	0.096
Interventricular septum (mm)	9.5 ± 1.1	9.0 ± 1.1	0.030
Posterior wall (mm)	8.0 ± 1.7	7.4 ± 1.4	0.125
End-diastolic diameter (mm)	52 ± 4	53 ± 4	0.451
Right ventricle			
End-diastolic volume (mL/m^2)	69 ± 13	64 ± 9	0.087
End-systolic volume (mL/m^2)	34 ± 9	30 ± 6	0.031
Ejection fraction (%)	52 ± 7	54 ± 6	0.202
Mass (g/m^2)	19 ± 6	19 ± 5	0.582
SA inflow tract diameter (mm)	46 ± 4	41 ± 5	<0.001
4C inflow tract diameter (mm)	46 ± 4	42 ± 5	0.001
Inflow tract area (cm^2)	22 ± 4	20 ± 3	0.050
Inflow tract end-diastolic volume (mL/m^2)	45 ± 10	40 ± 7	0.074
Inflow tract end-systolic volume (mL/m^2)	21 ± 6	19 ± 4	0.129
Inflow tract ejection fraction (%)	52 ± 11	53 ± 7	0.839
Outflow tract diameter (mm)	25 ± 3	25 ± 3	0.238
Outflow tract area (cm^2)	12 ± 2	12 ± 2	0.717
Outflow tract end-diastolic volume (mL/m^2)	25 ± 5	24 ± 4	0.528
Outflow tract end-systolic volume (mL/m^2)	13 ± 4	11 ± 3	0.047
Outflow tract ejection fraction (%)	49 ± 11	55 ± 10	0.032
TAPSE (mm)	23 ± 6	25 ± 5	0.093
Atria			
Left atrium area (cm^2)	19 ± 3	19 ± 4	0.928
Right atrium area (cm^2)	18 ± 4	17 ± 3	0.193

SA, short axis; 4C, four-chamber; TAPSE, tricuspidal annular plane systolic excursion.

$P < 0.001$) as well as in the four-chamber long-axis view (46 ± 4 vs. 42 ± 5 mm, $P = 0.001$) when compared with normal volunteers. In other terms, 14/30 (47%) and 9/30 (30%) BrS patients showed an RVIT diameter larger than the 75 and the 95 percentile of the controls, respectively. Area and volume measures confirmed a borderline enlargement of the RV inflow chamber in patients with the BrS (22 ± 4 vs. 20 ± 3 cm^2, $P = 0.050$; 45 ± 10 vs. 40 ± 7 mL/m^2, $P = 0.074$). Regional RVIT ejection fraction was not different between BrS patients and normal volunteers.

Conversely, RVOT was similar in the two groups of subjects in terms of diameter (25 ± 3 vs. 25 ± 3 mm; $P = 0.238$) as well as of area (12 ± 2 vs. 12 ± 2 cm^2; $P = 0.717$) and volume (25 ± 5 vs. 24 ± 4 mL/m^2, $P = 0.528$) but regional RVOT ejection fraction was lower in BrS patients (49 ± 11 vs. $55 \pm 10\%$; $P = 0.032$), because of an augmented RVOT ESV (13 ± 4 vs. 11 ± 3 mL/m^2; $P = 0.047$).

Among all dimensional and functional parameters listed in *Table 2*, only RVIT diameter was significantly different between BrS patients and normal volunteers after Bonferroni correction. Figure 4 depicts a representative BrS case with RVIT enlargement, compared to a control subject.

In the BrS group, the presence of enlarged RVIT, i.e. larger than the 75 percentile of the normal group values, did not correlate with the clinical presentation: family history of sudden death, history of syncope, spontaneous coved-type ECG pattern, AV or intraventricular conduction delay, or the presence of a mutation in the *SCN5A* gene.

Discussion

The BrS is a relatively frequent inherited arrhythmogenic syndrome. It is characterized by an electrocardiographic pattern of complete or incomplete RBBB and dynamic ST-segment elevation in the right precordial leads (V_1–V_3). The BrS was proposed as a new and distinct clinical entity in 1992 by Brugada and Brugada,[18] who described eight patients with a history of aborted sudden cardiac death owing to ventricular fibrillation, a typical electrocardiographic pattern and the absence of any structural heart disease. *SCN5A* gene encoding for the alpha subunit of the sodium channel gene has been associated with the phenotype of BrS and it represents the most prevalent genetic variant. More recently, other authors reported mutation on GPD1-L (glycerol-phosphate dehydrogenase-1 like),[19] and the cardiac calcium channel.[20]

Despite the original description of BrS excluded structural abnormalities, anecdotal observations on small patients' cohorts suggested the presence of RV abnormalities. Atrophy, fatty or fatty infiltration, at endomyocardial biopsy and/or autopsy, or morpho-functional abnormalities at echocardiography (dilatation and dysfunction) were also reported in the literature.[9,21] Furthermore,

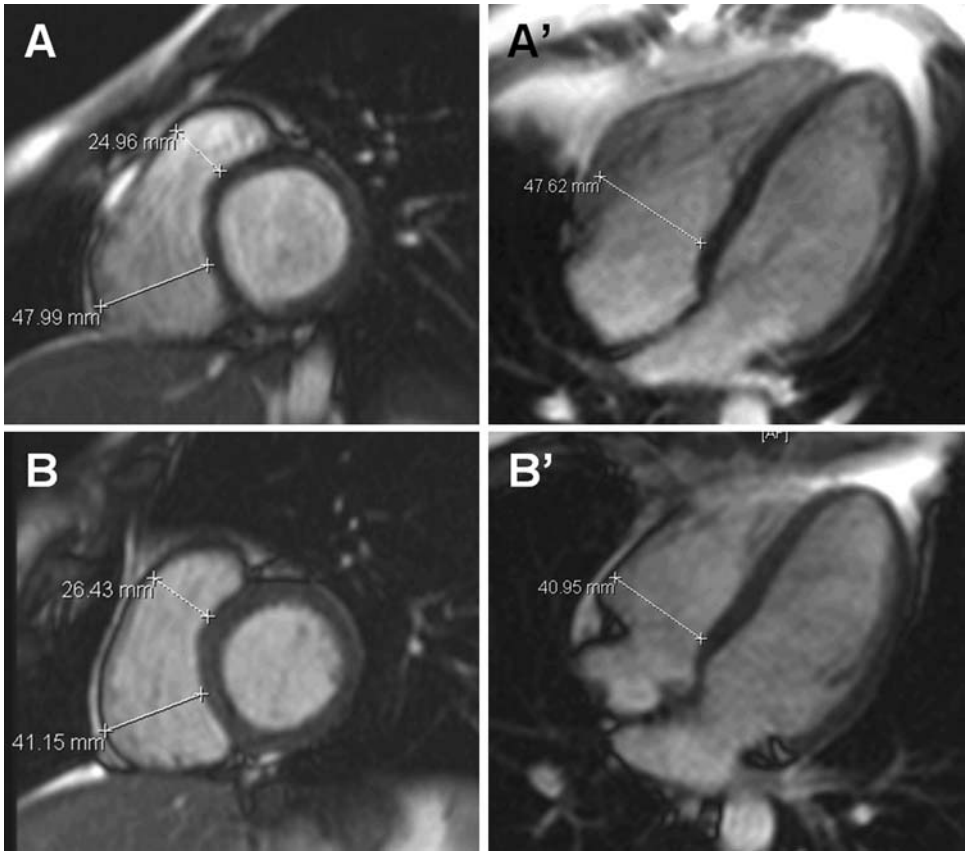

Figure 4 Right ventricle inflow tract dilatation in a patient with Brugada syndrome (*A* and *A'*), compared with normal RV diameters in a control patient (*B* and *B'*).

other authors suggested that ST-segment elevation in right precordial leads may be present in patients with ventricular fibrillation and RV cardiomyopathy.[10]

Diagnostic work out and follow-up of patients with BrS often includes transthoracic echocardiography (TTE) imaging, which has low sensitivity to detect RV abnormalities. Indeed, although TTE is sufficiently precise for the assessment of LV, it does not allow an accurate evaluation of the RV volumes and segmental contractility. Moreover, an adequate tissue characterization cannot be performed with TTE.

Wall motion abnormalities

Only one study has so far reported an abnormal contractility of the RV in the BrS patients. Using electron beam computed tomography, Takagi *et al.*[11] have observed wall motion abnormalities at the RVOT or, less frequently, at the RV inferior wall level in most of the 23 patients suffering from BrS with recent cardiac arrest or resuscitated sudden death.

Similar to the study of Takagi *et al.*, our data suggest the presence of RV contractility abnormalities in a clinically relevant percentage (50%) of BrS patients. Moreover, analysis of RV regional contractility shows an association between BrS diagnosis and a reduced contractility in the anterior-apical segment [$P = 0.041$; OR 6.8 (95% CI 1.1–41.7)], in the outflow, and borderline association with reduced contractility in the inferior mid-ventricular segment [$P = 0.051$; OR 4.92 (95% CI 1–24.4)] in the inflow.

Despite the unavoidable differences of the clinical characteristics of study cohorts, it is clear that the evidence supporting a structural involvement of the RV also determining mild wall motion abnormalities in this disease is accumulating.

Right ventricular enlargement

Papavassiliu *et al.*[14] have previously shown a significant enlargement of the RVOT area at CMRI in 20 BrS patients in comparison with age- and sex-matched normal controls.

In the present study, we did not find RVOT enlargement in BrS patients with respect to normal subjects. On the contrary, in our series of BrS patients, a significant enlargement of the RVIT diameter was detected both in the short-axis (46 ± 4 mm vs. 41 ± 5 mm; $P < 0.001$) and in the long-axis view (46 ± 4 vs. 42 ± 5; $P = 0.001$), and was the sole dimensional parameter significantly different after Bonferroni correction for multiple testing.

There are relevant methodological differences in the two studies: we used double-oblique cardiac-oriented views, sectioning RVOT with approximately the same angle with respect to its major axis; on the contrary Papavassiliu *et al.* measured RVOT on standard axial slices, then sectioning RVOT with an angle that varied according to the orientation of the heart in the chest. A more careful re-analysis of the study by Papavassiliu *et al.* highlights the presence of a larger RVIT diameter (EDD) among BrS patients, like in our study, on short-axis cardiac-oriented planes. Therefore, the discrepancy may be owing to methodological differences. Nonetheless, both studies (Papavassiliu and ours) clearly suggest that RV structural abnormalities may be present in some BrS patients (9/30 patients in our series).

Fatty infiltration

In the present study no fatty replacement of the RV was observed in any patient. Papavassiliu *et al.* reported this finding in 20% of the patients. It is unknown why the fatty replacement, frequently found at the endomyocardial biopsy or at post-mortem examination,[9,10] is rarely observed with CMRI. In normal hearts, fat is present on the epicardial surface of the RV and around the coronary blood vessels, in amount varying with an individual's age and sex.[22] Therefore, it is possible that the pathological meaning of bioptic or autoptic findings has been overestimated. Alternatively, fatty replacement might be present only in the most severe cases. Finally, a low rate of fat discovered in our study may derive from a more conservative approach to the problem, the RV wall being too thin (2–3 mm) to make robust statements on the real localization of fat (inside or outside the muscular wall).

Limitations of the study

Fibrotic replacement of the RV myocardium has been shown by delayed enhancement at CMR in small studies including patients with ARVC.[23,24] Delayed enhancement technique is proposed in the 'CMR Image acquisition Protocols' of the Society for Cardiovascular Magnetic Resonance for ARVC assessment. Our study was not originally designed to acquire this kind of information. Even if we took a conservative approach and we did not enrol patients having >1 major or >2 minor ARVC diagnosis criteria, or with ARVC diagnosis in relatives up to the second degree, this is a potential limitation of the study.

The radial fractional shortening method, we used to assess RV contractility, may not differentiate passive inward movement from active contraction of RV wall. Unfortunately, RV systolic myocardial thickening cannot be accurately assessed by CMRI (although it has good spatial resolution) owing to the very thin RV wall, and could not be considered as an alternative method.

Conclusions

In this study we carried out a detailed targeted morphological analysis of the RV in a consecutive cohort of BrS patients and we provide the final proof of concept that a clinically relevant percentage of BrS patient present with RV enlargement or mild wall motion abnormalities. As expected based on the 'electrical nature' of BrS, such abnormalities are of relatively small magnitude, but they are definitely present, as demonstrated with conditional logistic regression and supported by reproducibility analysis of our approach. Our findings are consistent and further refine previous data and suggest that BrS phenotype and pathophysiology are more complex than previously anticipated. We found no correlation between structural/motion abnormalities and the clinical presentation (family history of sudden death, history of syncope, spontaneous coved-type ECG pattern, AV or intraventricular conduction delay); however our study was not targeted to this endpoint and the relatively limited sample size could have hampered the statistical power to detect such correlation.

Furthermore, although it is well known that *SCN5A* mutations may be directly implicated in cardiomyopathies, such as

degenerative changes in the conduction system (Lenegre disease) and dilated cardiomyopathy,[25–27] we found no correlation between the presence of a sodium channel mutation and RV abnormalities in our patients. Once again our data point to the increasing complexity of the definition of BrS, which is the clinical expression of a non-uniform pathogenesis.

Nonetheless, our study has a direct clinical implication since it definitely proves the structural involvement of the RV in BrS and suggests the need of performing careful morphological assessment of the RV in all patients. It is currently unknown whether such structural abnormalities may worsen at follow-up if they may have a role in risk stratification. These issues should be the focus of future studies.

Supplementary material

Supplementary material is available at *European Heart Journal* online.

Funding

This work was supported by Telethon grants No. GGP04066 and GGP06007 and by funds from the Ministero dell' Università e della Ricerca Scientifica e Tecnologica: FIRB RBNE01XMP4_006, RBLA035A4X_002, PRIN 2006055828_002.

Conflict of interest: none declared.

References

1. Wilde AA, Antzelevitch C, Borggrefe M, Brugada J, Brugada R, Brugada P, Corrado D, Hauer RN, Kass RS, Nademanee K, Priori SG, Towbin JA, Study Group on the Molecular Basis of Arrhythmias of the European Society of Cardiology. Proposed diagnostic criteria for the Brugada syndrome. *Eur Heart J* 2002;**23**:1648–1654.
2. Antzelevitch C, Brugada P, Brugada J, Brugada R. Brugada syndrome: from cell to bedside. *Curr Probl Cardiol* 2005;**30**:9–54.
3. Antzelevitch C, Brugada P, Borggrefe M, Brugada J, Brugada R, Corrado D, Gussak I, LeMarec H, Nademanee K, Riera AR, Shimuzu W, Schulze-Bahr E, Tan H, Wilde A. Brugada syndrome: report of the second consensus conference. *Circulation* 2005;**111**:659–670.
4. Chen Q, Kirsch GE, Zhang D, Brugada R, Brugada J, Brugada P, Potenza D, Moya A, Borggrefe M, Breithardt G, Ortiz-Lopez R, Wang Z, Antzelevitch C, O'Brien RE, Schultze-Bahr E, Keating MT, Towbin JA, Wang Q. Genetic basis and molecular mechanisms for idiopathic ventricular fibrillation. *Nature* 1998;**392**:293–296.
5. Antzelevitch C. The Brugada syndrome: ionic basis and arrhythmia mechanisms. *J Cardiovasc Electrophysiol* 2001;**12**:268–272.
6. Priori SG, Napolitano C, Gasparini M, Pappone C, Della Bella P, Giordano U, Bloise R, Giustetto C, De Nardis R, Grillo M, Ronchetti E, Faggiano G, Nastoli J. Natural history of Brugada syndrome: insights for risk stratification and management. *Circulation* 2002;**105**:1342–1347.
7. Blaser JR. The cardiac sodium channel: gating function and molecular pharmacology. *J Mol Cell Cardiol* 2001;**33**:599–613.
8. Tan HL, Bezzina CR, Smits JP, Verkerk AO, Wilde AA. Genetic control of sodium channel function. *Cardiovasc Res* 2003;**57**:961–973.
9. Martini B, Nava A, Thiene G, Buja GF, Canciani B, Scognamiglio R, Daliento L, Dalla Volta S. Ventricular fibrillation without apparent heart disease: description of six cases. *Am Heart J* 1989;**118**:1203–1209.
10. Corrado D, Basso C, Buja GF, Nava A, Rossi L, Thiene G. Right bundle branch block, right precordiali ST-segment elevation and sudden death in young people. *Circulation* 2001;**103**:710–717.
11. Takagi M, Aihara N, Kuribayashi S, Taguchi A, Shimizu W, Kurita T, Suyama K, Kamakura S, Hamada S, Takamiya M. Localized right ventricular morphological abnormalities detected by electron-beam computed tomography represent arrhythmogenic substrates in patients with the Brugada syndrome. *Eur Heart J* 2001;**22**:1032–1041.
12. Takagi M, Aihara N, Kuribayashi S, Taguchi A, Kurita T, Suyama K, Kamakura S, Takamiya M. Abnormal response to sodium channel blockers in patients with Brugada syndrome: augmented localised wall motion abnormalities in the right ventricular outflow tract region detected by electron beam computed tomography. *Heart* 2003;**89**:169–174.
13. Frustaci A, Priori SG, Pieroni M, Chimenti C, Napolitano C, Rivolta I, Sanna T, Bellocci F, Russo MA. Cardiac histological substrate in patients with clinical phenotype of Brugada syndrome. *Circulation* 2005;**112**:3672–3674.
14. Papavassiliu T, Wolpert C, Flüchter S, Schimpf R, Neff W, Haase KK, Düber C, Borggrefe M. Magnetic resonance imaging findings in patients with Brugada syndrome. *J Cardiovasc Electrophysiol* 2004;**15**:1133–1138.
15. Jain A, Tandri H, Calkins H, Bluemke DA. Role of cardiovascular magnetic resonance imaging in arrhythmogenic right ventricular dysplasia. *J Cardiovasc Magn Reson* 2008;**10**:32.
16. Bellenger NG, Davies LC, Francis JM, Coats AJ, Pennell DJ. Reduction in sample size for studies of remodeling in heart failure by the use of cardiovascular magnetic resonance. *J Cardiovasc Magn Reson* 2000;**2**:271–278.
17. Bland JM, Altman DG. Agreement between methods of measurement with multiple observations per individual. *J Biopharm Stat* 2007;**17**:571–582.
18. Brugada P, Brugada J. Right bundle branch block, persistent ST segment elevation and sudden cardiac death: a distinct clinical and electrocardiographic syndrome. A multicenter report. *J Am Coll Cardiol* 1992;**20**:1391–1396.
19. London B, Michalec M, Mehdi H, Zhu X, Kerchner L, Sanyal S, Viswanathan PC, Pfahnl AE, Shang LL, Madhusudanan M, Baty CJ, Lagana S, Aleong R, Gutmann R, Ackerman MJ, McNamara DM, Weiss R, Dudley SC Jr. Mutation in glycerol-3-phosphate dehydrogenase 1 like gene (GPD1-L) decreases cardiac Na^+ current and causes inherited arrhythmias. *Circulation* 2007;**116**:2260–2268. Published online ahead of print 29 October 2007.
20. Antzelevitch C, Pollevick GD, Cordeiro JM, Casis O, Sanguinetti MC, Aizawa Y, Guerchicoff A, Pfeiffer R, Oliva A, Wollnik B, Gelber P, Bonaros EP Jr, Burashnikov E, Wu Y, Sargent JD, Schickel S, Oberheiden R, Bhatia A, Hsu LF, Haïssaguerre M, Schimpf R, Borggrefe M, Wolpert C. Loss-of-function mutations in the cardiac calcium channel underlie a new clinical entity characterized by ST-segment elevation, short QT intervals, and sudden cardiac death. *Circulation* 2007;**115**:442–449.
21. Corrado D, Nava A, Buja G, Martini B, Fasoli G, Oselladore L, Turrini P, Thiene G. Familial cardiomyopathy underlies syndrome of right bundle branch block, ST segment elevation and sudden death. *J Am Coll Cardiol* 1996;**27**:443–448.
22. Tansey DK, Aly Z, Sheppard MN. Fat in the right ventricle of the normal heart. *Histopathology* 2005;**46**:98–104.
23. Hunold P, Wieneke H, Bruder O, Krueger U, Schlosser T, Erbel R, Barkhausen J. Late enhancement: a new feature in MRI of arrhythmogenic right ventricular cardiomyopathy? *J Cardiovasc Magn Reson* 2005;**7**:649–655.
24. Tandri H, Saranathan M, Rodriguez ER, Martinez C, Bomma C, Nasir K, Rosen B, Lima JA, Calkins H, Bluemke DA. Non-invasive detection of myocardial fibrosis in arrhythmogenic right ventricular cardiomyopathy using delayed-enhancement magnetic resonance imaging. *J Am Coll Cardiol* 2005;**45**:98–103.
25. Schott JJ, Alshinawi C, Kyndt F, Probst V, Hoorntje TM, Hulsbeek M, Wilde AA, Escande D, Mannens MM, Le Marec H. Cardiac conduction defects associate with mutations in *SCN5A*. *Nat Genet* 1999;**23**:20–21.
26. Olson TM, Michels VV, Ballew JD, Reyna SP, Karst ML, Herron KJ, Horton SC, Rodeheffer RJ, Anderson JL. Sodium channel mutations and susceptibility to heart failure and atrial fibrillation. *JAMA* 2005;**293**:447–454.
27. McNair WP, Ku L, Taylor MR, Fain PR, Dao D, Wolfel E, Mestroni L. SCN5A mutation associated with dilated cardiomyopathy, conduction disorder, and arrhythmia. *Circulation* 2004;**110**:2163–2167.